# A chemical kinetic perspective on the low-temperature oxidation of propane/propene mixtures through experiments and kinetic analyses

Ajoy Ramalingam[*1], Snehasish Panigrahy[2], Yann Fenard[1,3], Henry Curran[2], Karl Alexander Heufer[1,4]

[1] *Physico-Chemical Fundamentals of Combustion (PCFC), RWTH Aachen University, 52056 Aachen, Germany*

[2] *Combustion Chemistry Center (C$^3$), National University of Ireland Galway, Republic of Ireland*

[3] *Physicochimie des Processus de Combustion et de l'Atmosphère (PC2A), F-59000 Lille, France*

[4] *Hochdruck-Gasdynamik (HGD), RWTH Aachen University, 52056 Aachen, Germany*

[*]**Corresponding author**: ramalingam@pcfc.rwth-aachen.de

**Address:** Physico-Chemical Fundamentals of Combustion (PCFC)

Schinkelstraße 8, Fuel Science Center, RWTH Aachen University,

52062 Aachen, Germany

## Abstract

In recent years, our understanding of fuel oxidation has improved with rigorous experimental and theoretical investigations being performed. As investigation methods evolve, our understanding of fundamental fuel chemistry advances. This process allows us to revisit and improve our existing chemical kinetic models. Propane and propene have been studied in various facilities at different conditions; however, the interaction of these two species has not been explored well. These two species play a crucial role in the oxidation of larger hydrocarbons and constitute a significant fraction of liquefied petroleum gas. The current study involves an experimental investigation of ignition delay time measurements for neat propene and propane/propene (50%/50%) mixtures in a rapid compression machine for a range of pressures (20–80 bar). These auto-ignition experiments are complemented by the measurement of stable intermediate species mole fraction profiles at 750 K for the non-diluted stoichiometric condition at 40 bar and 50 bar. The experimental output from this study has contributed to the development of NUIGMech1.0 at high-pressure conditions, for mixtures that are relevant to engine applications. NUIGMech1.0 is utilized for the kinetic analysis, and its performance is also compared with two other relevant mechanisms. The kinetic analysis is used to establish an understanding of the fundamental chemistry controlling fuel oxidation and also to provide updates of the chemical kinetic mechanism. Additionally, the critical reaction pathways and sensitive reactions that lead to the intermediate species that control reactivity are explained in detail. It is found that cross-reactions from both the propane and propene sub-mechanisms play a crucial role in controlling the reactivity of the mixtures. NUIGMech1.0 not only captures the reactivity and speciation data for the neat components but also shows good predictions of the mixtures at the conditions studied.

## Keywords
Propene, Propane/Propene mixtures, ignition delay time, sampling study, rapid compression machine

## 1. Introduction

Fuels such as natural gas and liquefied petroleum gas (LPG) are being considered as alternative fuels as they reduce $CO_2$ emissions compared to their gasoline/diesel counterparts. Secondly, these fuels can also be produced through carbon-neutral processes coupled with power-to-gas [1] and bio-methane production processes [2, 3]. They have long been investigated for applications in road and sea transportation, but now, fuels like liquid methane and propene are being tested for use in commercial space transportation [4, 5]. The development of these engines for different applications requires immense prototyping and testing. However, with the recent trends in computational capabilities and advances in powertrain simulations, it is possible to reduce the effort spent on prototyping and testing. From this perspective, knowledge of emissions and ignition behavior of different fuels can be obtained through chemical kinetic mechanisms. The ability of a mechanism to predict different application relevant conditions is vital in this process. Therefore, understanding the oxidation of these fuels on a fundamental level is essential to accurate reactivity predictions. Although there are investigations on the lower hydrocarbons in the literature, there is still a lack of mechanistic data for fuel mixtures at application relevant pressures.

Propene and propane are significant components of LPG [6-9], and they also serve as representative species for larger alkanes and alkenes. Therefore, investigating these species and their mixtures can provide new insights into their oxidation behavior and lead to a mechanism that can capture the auto-ignition behavior of LPG fuels containing significant concentrations of propane and propene. A pressure-temperature plot showing available literature data for propane was presented in a recent study [10]. Moreover, a detailed review is also available in studies by Goldsborough et al. [11] and Sabia et al. [12]. The recent work by Burke et al. [13, 14] investigated propene in different facilities for a wide range of conditions and provided a detailed review of other propene studies in the literature. Burke et al. [13, 14] also developed a detailed kinetic mechanism describing propene oxidation; however, there is a quantitative gap in the ability of the mechanism to replicate experimental data for propane and for propane/propene mixtures. Apart from a recent study by Ramalingam et al. [9] of different automotive LPG fuels, there is still a great void in experimental data for propane/propene mixtures. **Figure 1** shows the pressure-temperature plot for propene experiments that are available in the literature from different facilities [13-27].

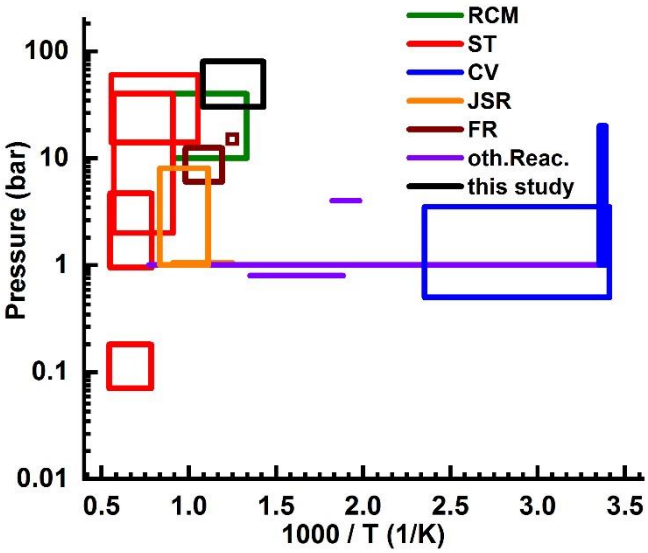


**Figure 1: A pressure vs. temperature plot of propene investigations with different reactors (RCM- rapid compression machine, ST- Shock tube, CV- Combustion vessel, JSR- Jet-stirred reactor, FR- flow reactor) from the literature.**

The primary goal of this study is to develop a consistent mechanism that can represent the auto-ignition behavior of propane, propene, and their mixtures over a wide range of temperature, pressure, mixture composition, and dilution. The mechanism development is a continually evolving process, and the experimental work established in this work and from previous studies [9, 10] has contributed to the development of NUIGMech1.0. The study on automotive LPG fuels [9] and the previous study on propane [10] showed that mechanisms available in the literature do not capture the reactivity for the neat components and their mixtures in a consistent way. In this study, the experimental work on propene is extended to higher pressures (80 bar) for stoichiometric mixtures in a rapid compression machine (RCM). Propane/propene mixtures are also studied for a range of pressures (20–60 bar) at stoichiometric conditions. A speciation study for propane/propene mixtures and neat propene is performed at 750 K for compressed pressures of 40 bar and 50 bar, respectively. Recent work on species produced during the oxidation of propane in the RCM [10] was also performed at the same compressed temperature, and therefore allows for a comparison of propane, propene, and their mixtures using the ignition delay time (IDT) and speciation results. To the authors' knowledge, this is the first study to obtain experimental IDT and speciation data for propene and propane/propene mixtures at high pressures.

# 2. Experimental description

## 2.1 Ignition delay time measurements

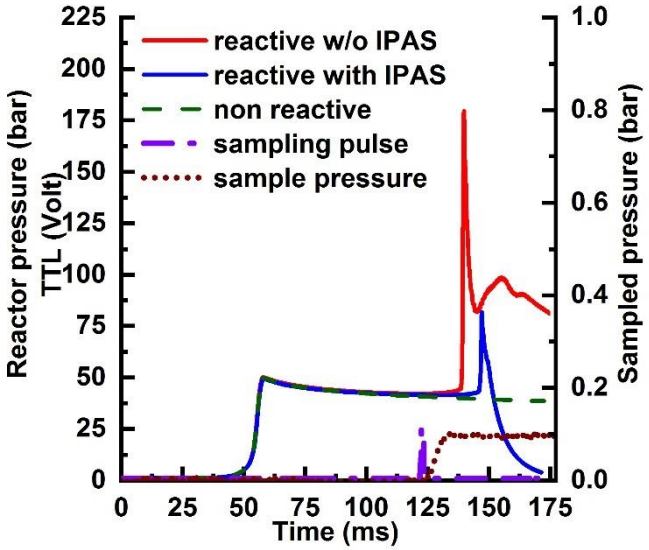


**Figure 2: Recorded experimental traces from an IDT and sampling experiment (propene, $p_C$= 50 bar, $\varphi$ = 1, $T_C$ = 750 K, diluent = 75.48%).**

The high-pressure IDT measurements were performed in the RCM at PCFC, RWTH Aachen University. The description of the facility is provided in previous studies [28, 29]. In brief, the single stroke creviced piston is pneumatically driven and hydraulically stopped. The compressed temperature is varied using different diluent gas ratios or by varying the compression ratio using different end wall positions [29]. The heating of the mixture tank, manifold, and the reaction chamber is controlled and monitored using type-T thermocouples. The mixture is prepared by monitoring the partial pressures using two static pressure sensors (ATM STS 1$^{st}$: 0–0.5 bar, ATM STS 1$^{st}$: 0–5 bar). The reactive and non-reactive mixtures were prepared using high purity grade propene (99.95%), propane (99.95%), nitrogen (99.999%), argon (99.996%), carbon dioxide (99.5%), and oxygen (99.999%). For the relatively low-pressure experiments (< 50 bar), the dynamic pressure in the reactor is monitored using a Kistler 6125C11U20 pressure sensor. However, for the high-pressure experiments (> 50 bar) investigated in this study, the dynamic pressure was monitored using a PCB 113B22 pressure sensor for the reactive experiments, and both a Kistler 6125C11U20 and PCB 113B22 pressure sensors were used in tandem for the non-reactive experiments. The measured pressure by PCB 113B22 is lower than the actual pressure as it is affected by thermal heat-shock. The non-reactive pressure traces from both sensors are used to correct the pressure for the reactive experiment, and in turn, the corrected pressure is used to estimate the compressed temperature using Gaseq [30]. This procedure is explained in detail in the work by Ramalingam et al. [29]. A reference pressure trace for a reactive and non-reactive experiment is provided in **Figure 2**. The pressure fluctuation after the main ignition in the reactive pressure trace without IPAS is a consequence of different effects. Globally, the pressure level is decreasing after ignition due to heat loss effects. However, pressure fluctuations can result from piston rebound or strong pressure waves induced by the ignition, which propagates and reflects several times at the walls. Nevertheless, this pressure fluctuation does not affect the result of the experiments. The non-reactive pressure time histories for the different experiments are converted into effective volume time histories that are used as input files in our simulations [11, 31]. The procedure to perform the high-pressure experiments in the RCM and estimate their experimental uncertainties is elaborated in a previous study [29]. The estimated uncertainty in the compressed temperature is ± 5 K, and the observed variation in the compressed pressure is less than 2%. The variation in the measured IDT is within 20%, which is similar to other studies in the literature [13].

## 2.2 Speciation measurements

The speciation measurements for propene and the propane/propene mixtures were also performed in the PCFC RCM. The extracted sample was analyzed using a gas chromatograph and mass spectrometer equipped with a flame ionization detector system (GCMS/FID). A detailed description and schematic of the sampling system are provided in a previous paper [10]. In brief, the sampling system consists of a fixed compression ratio endwall with a conical protruding tube, a fast-acting valve, a sampling volume, a syringe system, and the ignition peak avoidance system (IPAS). The conical protruding tube on the endwall surface faces the inner side of the reaction chamber and aids in extracting a sample from the reaction core. The fast-acting solenoid valve (Parker series 9) is mounted to the outer surface of the endwall and connected to a sampling volume (~ 7.5 ml) and a sample transfer system. The sample transfer system consists of a stainless-steel syringe with a Kulite pressure sensor mounted on its piston. The fast-acting solenoid valve is triggered using the pressure signal from the reactor, a digital delay generator (Stanford systems), and an IOTA pulse driver (Parker). The triggering pulse width is set to 1 ms on the IOTA pulse driver. The signal from the reactor pressure sensor, the triggered pulse width, and the sampled pressure traces are recorded on a computer. The high-pressure IDT experiments involve intense peak pressures that are typically above the rated pressure of the fast-acting solenoid valve. The IPAS system is connected to one of the six ports in the reaction chamber to avoid intense peak pressures from damaging the solenoid valve. The IPAS system consists of a thin diaphragm that separates the reaction chamber from a large volume, and during the ignition process, the diaphragm breaks, rapidly reducing the pressure in the reaction chamber. **Figure 2** shows the pressure trace during the sampling experiment. Once the sample is extracted from the reaction core, the sample is transferred to the GCMS/FID system.

The GCMS/FID system consists of a Porabond PLOT Q column used to separate the oxygenated and hydrocarbon species. The column is connected to both the FID and the MS system. The MS is used to identify the species, whereas the FID chromatogram quantifies the different species. The species identified in the current work were calibrated using calibration gas standards obtained from Westfalen AG and Praxair Germany GmbH. For the non-calibrated species identified, the equivalent carbon number method was used. The response factor for each identified species is used to quantify the measured mole fractions of each experiment. The measured mole fractions are plotted against the normalized time, where '0' denotes the end of compression time, and '1' denotes the time of ignition. It is important to note that the desired gas sampling from the core of the reactor is influenced by the gas in the dead volume of the protruded tube. The dead volume has a large surface area-to-volume ratio, which leads to chemical quenching of the compressed gases, and therefore, lowers the temperature in this volume. Consequently, once the fast-acting valve is triggered to open, this unreacted gas is also sampled along with the extracted sample from the reaction core. This process dilutes the entire sample and has to be corrected using a dilution factor. This method of correcting the dilution is quite common in this sampling technique and thus is not elaborated upon here [10, 32-35].

The uncertainty in the sampling experiments is explained in detail in the previous work [10]. Hence, only our estimated values are presented in this work. The variation in IDTs for the speciation measurements for the propane/propene and propene mixtures at 40 and 50 bar are 52.5 ± 1.5 ms and 89 ± 1.5 ms, respectively. A time scale uncertainty is induced by the opening and closing behavior of the valve. The sampling period variation is 1.470 ± 0.070 ms and 1.634 ± 0.135 ms for the 40 and 50 bar experiments, respectively. The uncertainty in the mole fraction scale is induced by the variation in the response factor, the uncertainty for correction of the dilution effect, uncertainty in the compressed temperature, variation arising from the sampling period. The overall uncertainty in the mole fraction scale is estimated to be 19% and 26% for the calibrated and non-calibrated species, respectively. Apart from these influences on the uncertainty in the mole fraction scale, the simulation method adds another 3% uncertainty induced by the impact of dead volume in the reaction chamber (i.e., crevice volume, IPAS dead volume, reactor inlet connection dead volume).

## 3. Computation methods

The IDT simulations were performed using NUIGMech1.0 with non-reactive input files. For each reactive experimental temperature obtained, a non-reactive experiment is performed by replacing the oxygen content with nitrogen. The non-reactive pressure traces obtained are converted into effective volume traces using the isentropic relationship. The effective volume traces, together with the initial experimental conditions, are used to perform zero-dimensional simulations [11, 31]. The simulation of IDTs, species mole fraction profiles, sensitivity, and rate of production analyses were all performed using an in-house script developed using Cantera [36]. The input files used for the simulations are provided as **Supplementary material (SM)**.

For the simulation of the speciation profiles, the IDT simulations are adapted to provide species-time histories during the ignition delay period. The procedure of normalization is also implemented for comparison against the experimental data. In a previous work [10], different computational methodologies to simulate species profiles were discussed, and therefore, more details are not provided here. The sensitivity and rate of production analyses were performed using a constant volume reactor, and these are used to identify the most sensitive reactions and pathways leading to key intermediates controlling fuel reactivity.

## 4. Model development, comparison, and kinetic analysis

In the introduction, we indicated that the goal of this work is to obtain a consistent mechanism that can predict both the neat components of propane and propene, along with their mixtures in the investigated regime. For this purpose, many mechanisms from the literature were considered, and simulations against the high-pressure IDT experiments for propane [10] and four different automotive LPG mixtures [9] were performed and analyzed. At the same time, the recent study by Burke et al. [13, 14] investigated the oxidation of propene for a wide range of experimental conditions using different reactors and established a mechanism that represents the oxidation of propene well. The development of NUIGMech1.0 is a large undertaking with contributions from several experimental [9, 10, 37-40] and theoretical studies [41-44], of which a few are referenced here. NUIGMech1.0 is hierarchically developed from hydrogen/oxygen to *n*-heptane chemistry. The detailed model contains 11260 elementary reactions and 2845 chemical species. In this work, only the base mechanism up to $C_3$ species chemistry is considered, and the collaborative effort from both groups has led to the development of a consistent propane/propene mechanism described in detail here. The mechanism used for this purpose, along with the glossary, is provided as **SM**.

### 4.1 Propene

The two-part study from Burke et al. [13, 14] approached propene oxidation with experimental investigations for a wide range of conditions to obtain species information from flow reactors and jet-stirred reactors, while simultaneously obtaining information on global parameters such as IDT and laminar burning velocities from shock tubes (STs), RCMs, and combustion vessels, respectively. The model developed as part of the study [13, 14] could represent most of the measured data from the different reactors with some shortcomings in the species mole fraction profiles. Although species profiles at comparatively higher pressures exist in their study [14] and from the literature [18], these investigations were performed at diluted conditions. As the sensitivity of some critical reaction pathways can vary depending on the percentage dilution of a mixture [10], species information at non-diluted conditions can provide another degree of constraint on a mechanisms' ability to predict different conditions. Therefore, in this study, IDTs for propene oxidation were obtained at pressures ranging from 30 to 80 bar in the RCM. In addition to the IDT data, information on species mole fractions has been obtained for propene at 750 K and non-diluted stoichiometric conditions. The mechanism from Burke et al. [13, 14], AramcoMech3.0 [45], and the recently developed NUIGMech1.0 are used for the simulation and kinetic analyses. **Figure 3(a)** compares the performance of the three selected mechanisms against our IDT measurements. **Figure 3(b)** shows a

comparison of sensitivity analyses of chemical reactions to IDT measurements for 50 bar, 750 K, and stoichiometric conditions, while **Figure 3(c)** shows reaction pathway analyses performed at the time when 10% of the fuel is consumed using the selected mechanism at the sampling condition. The stable intermediate species quantified in the measurements are highlighted using rectangles **(Figure 3(c))**. The species nomenclature is provided in the glossary and for the discussion in the different sections, the species molecular structure can be referred in the reaction pathway analyses. The discussion of propene oxidation is provided using the species mole fraction profiles and the kinetic analysis using NUIGMech1.0.

AramcoMech3.0 [45] over-predicts IDTs for propene and, therefore, is not considered for the kinetic analysis in this section, **Fig. 3(a)**. Both the Burke et al. [13, 14] and NUIGMech1.0 mechanisms show good agreement with the data and are well within the experimental uncertainties. However, the former is moderately more reactive than the latter. Both the experimental data and the simulation results show a moderate change in reactivity at temperatures below 870 K, and the mechanisms can capture this trend reasonably well. With the data obtained in the study by Burke et al. [13, 14] and the data from this study, the measurement envelope is increased to 80 bar pressure for stoichiometric conditions NUIGMech1.0 can predict well the reactivity and the pressure dependency in this range. The sensitivity analyses performed for the different pressures at 800 K **(Fig. S1)** show sensitive reactions observed in **Fig. 3(b).** However, the ranking of the sensitive reactions changes marginally with pressure **(Fig. S1)**. Comparing the two selected mechanisms with the IDT and species mole fraction profiles for propene oxidation is a classic example illustrating the importance of species measurements at application relevant conditions, **Fig. 4**. The global parameter, in this case, IDT, is captured well by both mechanisms, but the species mole fraction profiles alter this perspective. Even though the Burke et al. [13, 14] mechanism was able to predict the speciation trends in the flow- and jet-stirred reactor measurements reasonably well, the contrast in the prediction capabilities in the application relevant conditions is quite visible. Further discussions will present the differences in the mechanisms and, at the same time, provide an understanding of propene oxidation.

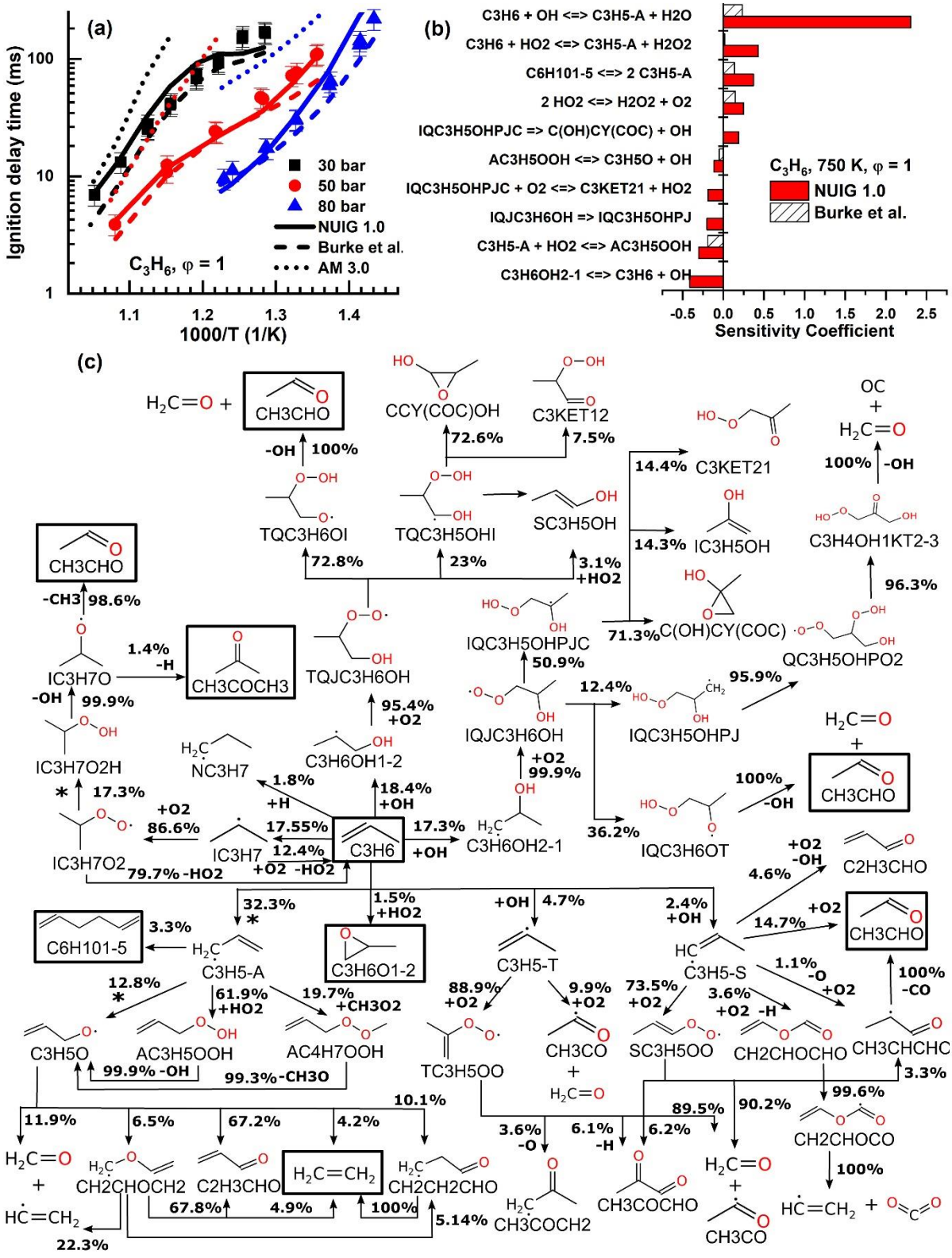


**Figure 3 (a) Performance comparison of NUIGMech1.0 and the mechanism from Burke et al. [13, 14] with experimental IDTs at 30, 50, and 80 bar for stoichiometric conditions, (Exp. – Symbols, Simulations – Lines). (b) Sensitivity analysis to IDT using NUIGMech1.0 and the mechanism from Burke et al. [13, 14] for non-diluted stoichiometric propene/air mixtures at 750 K and 50 bar. (c) Rate of production analysis using NUIGMech1.0 at 10% of fuel consumption at conditions same as (b). Species indicated inside the rectangle are observed and quantified in the sampling experiments.**

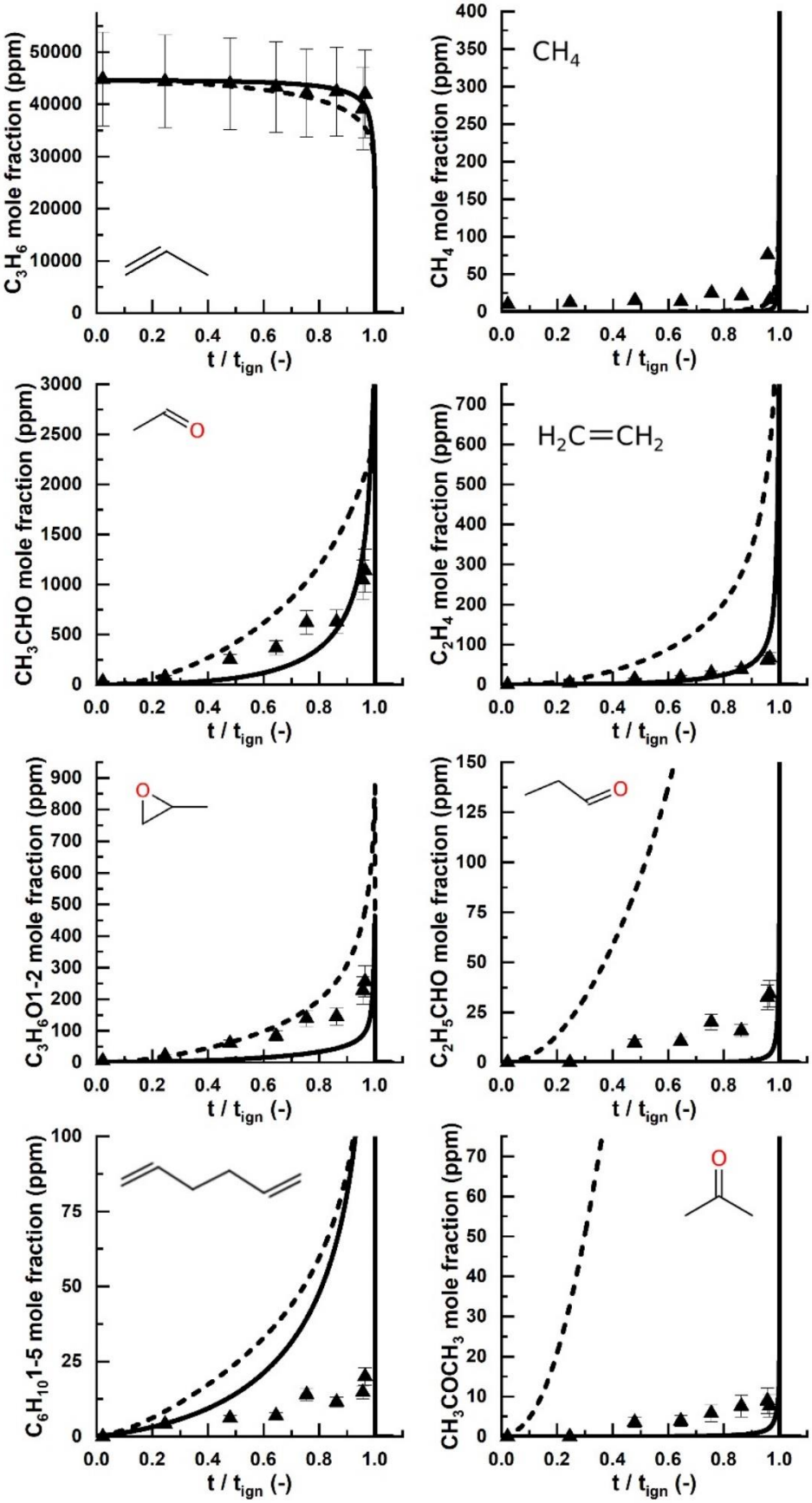


**Figure 4: Comparison of NUIGMech1.0 and the mechanism from Burke et al. [13, 14] against the intermediate species mole fraction profiles for propene oxidation at 750 K, 50 bar, and stoichiometric mixtures (Exp – symbols, Solid line – NUIGMech1.0, dashed line – Burke et al.).**

The rate of production analysis reveals that the primary consumption pathway for propene is through the hydroxyl (ȮH) radical, forming the resonantly stabilized allyl radical ($\dot{C}_3H_5$-a). The rate constants for H-atom abstraction from the allylic site by ȮH radical is based on the experimental work of Badra et al. [46], where the rate coefficients were directly measured in ST measurements over the temperature range of 818–1460 K. Bott and Cohen [47] also investigated this reaction with the help of shock tube experiments at 1 atm and 1200 K using UV absorption to measure ȮH concentrations. Zádor et al. [48] calculated this rate constant theoretically, which is in reasonable agreement with the measured rate by Badra et al. [46] at low-temperatures (800–910 K). However, the theoretical rate starts to deviate from the experimental data by a factor of two at higher temperatures (> 910 K), Error! Reference source not found.**(b)**. In NUIGMech1.0, a fit to both the experimental studies [46, 47] was implemented. The formation of the allyl radicals through H-atom abstraction from propene by molecular oxygen has been optimized. The reaction rate from Zhou et al. [49] matches the experimental measurements from Stothard et al. [50] and Barbe et al. [51] in the temperature range from 600-900 K (**Fig. 5(a)**). The rate used in NUIGMech1.0 is tailored to be faster by a factor of three compared to the rate from Zhou et al. [49] in order to match the IDT data in the intermediate and low-temperature regimes. The other leading consumption pathways are the addition of ȮH radicals to propene forming 1-hydroxy-propan-2-yl ($\dot{C}_3H_6OH1$-2) and 2-hydroxy-propan-1-yl ($\dot{C}_3H_6OH2$-1) radicals. The branching ratios of both the latter pathways were changed based on the work of Zádor and Miller [52] in NUIGMech1.0. The pathway leading to the production of allyl radicals is very sensitive and inhibits reactivity in NUIGMech1.0. At the same time, this reaction and the pathways leading to $\dot{C}_3H_6OH1$-2 and $\dot{C}_3H_6OH2$-1 radicals promote reactivity but are not seen to be sensitive in the Burke et al. mechanism [13, 14], **Fig. 3(b)**. The reason for the stark variations in these sensitivities, **Fig. 3(b)** is associated with changes in the flux during primary fuel consumption ($C_3H_6 + ȮH \leftrightarrow \dot{C}_3H_5$-a $+ H_2O$, $C_3H_6 + HȮ_2 \leftrightarrow \dot{C}_3H_5$-a $+ H_2O_2$, $C_3H_6 + ȮH \leftrightarrow \dot{C}_3H_6OH2$-1). The molecular additions of oxygen to $\dot{C}_3H_6OH1$-2 and $\dot{C}_3H_6OH2$-1 radicals have been updated from Miyoshi [53]. The subsequent pathways at this stage play a crucial role in controlling the reactivity and also in predicting the production of other stable intermediate species.

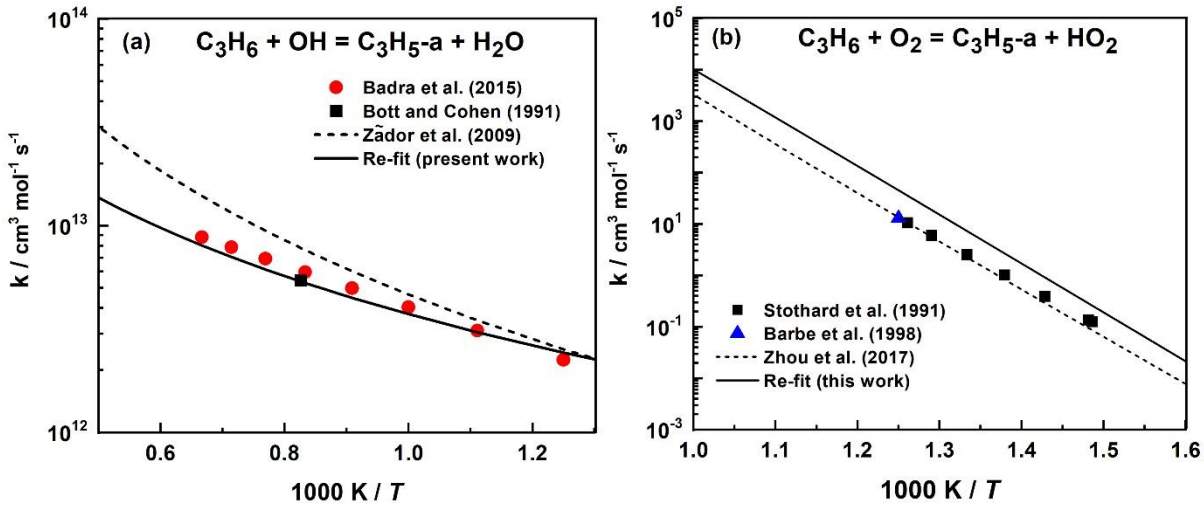


**Figure 5: Rate constant comparison of allylic H-atom abstraction from $C_3H_6$ by (a) $O_2$ and (b) ȮH, respectively.**

The fuel consumption is well predicted by both mechanisms compared to the experimental data and its associated uncertainty. However, with the Burke et al. [13, 14] mechanism, the fuel is moderately more consumed than the predictions using NUIGMech1.0, which leads to an overestimation of the stable intermediate species, **Fig. 4**. This effect is also reflected in the reactivity of propene at 750 K and 50 bar, **Fig. 3(a)**. The formation of ethylene is mainly controlled by the decomposition of allyloxy radicals ($C_3H_5Ȯ$). The isomerization reaction of allyloxy radicals to $ĊH_2CHOCH_2$ and $ĊH_2CH_2CHO$ radicals further contribute to the formation of ethylene. From sensitivity

analysis, it can be observed that the pathways leading to the formation of allyl hydroperoxide ($aC_3H_5OOH$) from allyl radicals, and the subsequent decomposition of allyl hydroperoxide to allyloxy radicals promote reactivity. This effect can be reasoned by the consumption of less reactive hydroperoxyl ($H\dot{O}_2$) radicals from the radical pool and the production of more reactive $\dot{O}H$ radicals during the reaction sequence. The species mole fraction profiles of ethene have improved in the right direction, with NUIGMech1.0 capturing the trend reasonably well.

Acetaldehyde ($CH_3CHO$) is another important intermediate produced during the oxidation of propene. It is formed through the Waddington mechanism and has been revised in NUIGMech1.0 based on the study of Lizardo-Huerta et al. [54]. The Waddington mechanism was not adequately included in the mechanism by Burke et al. [13, 14]. First, the addition of 2-hydroxyl-propan-1-yl ($\dot{C}_3H_6OH2\text{-}1$) radicals to $O_2$ and the subsequent Waddington mechanism reactions were not included in that mechanism. Moreover, only a single step Waddington mechanism for 1-hydroxyl-propan-2-yl peroxy was present. In the current model, two-step Waddington mechanisms for both 2-hydroxyl-propan-1-yl peroxy and 1-hydroxyl-propan-2-yl peroxy radicals are included, where in the first step, the hydroxyl H-atom to the peroxyl function of $TQJC_3H_6OH$ undergoes an internal H-atom transfer to form $TQC_3H_6OI$. In the second step, propoxyl-hydroperoxide radicals readily undergo β-scission, while hydroperoxyl-propyl radicals decompose to form acetaldehyde and hydroxyl radicals ($TQC_3H_6OI$ => $CH_2O + CH_3CHO + \dot{O}H$). The inclusion of the missing Waddington pathways has led to an improved prediction of acetaldehyde in the species mole fraction profiles. Furthermore, $\dot{H}$ atom addition to propene producing *iso*-propyl radicals, and the subsequent pathways leading to the production of acetaldehyde through the scission of $iC_3H_7\dot{O}$ radicals are another contributing pathway. These updates have improved the prediction of acetaldehyde mole fraction profiles compared to those predicted using the Burke et al. mechanism [13, 14].

Propanal ($C_2H_5CHO$) is another important aldehyde detected, which is facilitated through the formic acid-catalyzed conversion of prop-1-en-1-ol ($sC_3H_5OH$). Propanal is also produced from the addition reaction of molecular oxygen to *n*-propoxyl radicals ($nC_3H_7\dot{O} + O_2 \leftrightarrow C_2H_5CHO + H\dot{O}_2$). In NUIGMech1.0, the rate constant for this reaction is adopted from Zabarnick and Heicklen [55] and is two times lower than the estimated rate used by Burke et al. [9, 10]. These modifications have led to the under-prediction of propanal in NUIGMech1.0.

Another intermediate species over-predicted by the Burke et al. mechanism [13, 14] is acetone ($CH_3COCH_3$). The production of acetone was guided by the addition of oxygen to $\dot{C}_3H_6OH2\text{-}1$ radicals. The Waddington pathways in NUIGMech1.0 has changed the fluxes that have led to the channels promoting ($IQJC_3H_6OH \rightleftharpoons IQC_3H_5OHPJ$, $IQC_3H_5OHPJC + O_2 \leftrightarrow C_3KET21 + H\dot{O}_2$) and inhibiting ($IQC_3H_5OHPJC \rightarrow C(OH)CY(COC) + \dot{O}H$) the reactivity. Based on the theoretical calculation by Lizardo-Huerta et al. [54], the rate constant of $IQJC_3H_6OH \rightleftharpoons IQC_3H_5OHPJC$ is higher than that of $IQJC_3H_6OH \rightleftharpoons IQC_3H_6OT$ above 800 K. Thus, the significant percentage of flux from $IQJC_3H_6OH$ forms $IQC_3H_5OHPJC$ (50.9%) and about 36% of $IQJC_3H_6OH$ undergo H-atom rearrangement to form IQC3H6OT and the remaining produce $IQC_3H_5OHPJ$. In NUIGMech1.0, the production channels have been optimized, and the primary channel for the production of acetone is from the dissociation of $iC_3H_7\dot{O}$ radicals forming $CH_3COCH_3 + \dot{H}$ atoms. Previously, an estimated rate constant for *iso*-propoxy radical decomposition was included in the mechanism published by Burke et al. [13, 14]. In the present work, pressure-dependent rate coefficients for the unimolecular dissociation reaction have been derived from the recent calculations of Zádor and Miller [52].

The two other intermediates detected in the experiments are propylene oxide ($C_3H_6O1\text{-}2$) and 1,5-hexadiene ($C_6H_{10}1\text{-}5$), both formed very early in the fuel oxidation scheme. Propylene oxide is formed from the addition of $H\dot{O}_2$ radicals to propene, and the 1,5-hexadiene is formed through the recombination of allyl radicals. The hydroperoxyl-alkyl radicals ($\dot{C}_3H_6OOH1\text{-}2$, $\dot{C}_3H_6OOH2\text{-}1$) also undergo β-scission reactions to form propylene oxide. In the case of 1,5-hexadiene, the recombination of allyl radicals is sensitive in constraining the reactivity due to the formation of more unsaturated species in its reaction scheme. The mechanism under-predicts the species mole fraction profile of propylene oxide by a factor of two and over-predicts the 1,5-hexadiene mole fraction profile by ten at

the normalized time of 0.8. The optimization of the production routes of propylene oxide and 1,5-hexadiene would affect the mechanism's prediction capability at other reactor conditions.

Additionally, small quantities of acetylene, 1,3-butadiene, 2-propen-1-ol, and 3-methoxypropene were observed in the signals from the MS for experiments close to the normalized ignition point. On the other hand, the simulations also show significant quantities of 2-methyloxiran-2-ol (C(OH)CY(COC)), 3-methyloxiran-2-ol (CCY(COC)OH), and acrolein ($C_2H_3CHO$) at the region closer to ignition. However, these species were not observed in the experimental analysis. The consumption pathways of 2- and 3-methyloxiran-2-ol species are not very well established, and similar to other three-membered cyclic ether species, they could also possibly undergo isomerization reactions at comparatively lower temperatures [56-58].

## 4.2 Propane/propene

In the current study, the reactivity for stoichiometric propane/propene mixtures was determined in the temperature range 735–950 K at pressures of 20, 40, and 60 bar. To constrain the experimental matrix, and therefore the validation targets, the speciation measurements were performed at 40 bar. However, the temperature at the point of interest was kept at 750 K. In the following discussion, the kinetic analysis will be described with three mechanisms, namely NUIGMech1.0**,** AramcoMech3.0 [45]**,** and the mechanism from Burke et al. [13, 14]**. Fig. 6(a), (b), and (c)** show the IDT measurements and simulations using the three mechanisms, the sensitivity analysis at the point of interest (750 K) using the three mechanisms, and the reaction pathway analysis using NUIGMech1.0 at 10% fuel consumed (i.e., in the case of the current analysis 10% propane consumption was considered). The mole fraction species profiles for the mixtures are presented in **Fig. 7**, where the three mechanisms are compared against the measured experimental data. As before, the kinetic analysis will elaborate on the crucial pathways leading to the production of the stable intermediates and also establish the pathways that control the reactivity in the investigated regime. The propene sub-chemistry updates implemented in NUIGMech1.0 have been elaborated in the previous section, and the optimization performed for propane sub-chemistry will be described in this section along with the analysis.

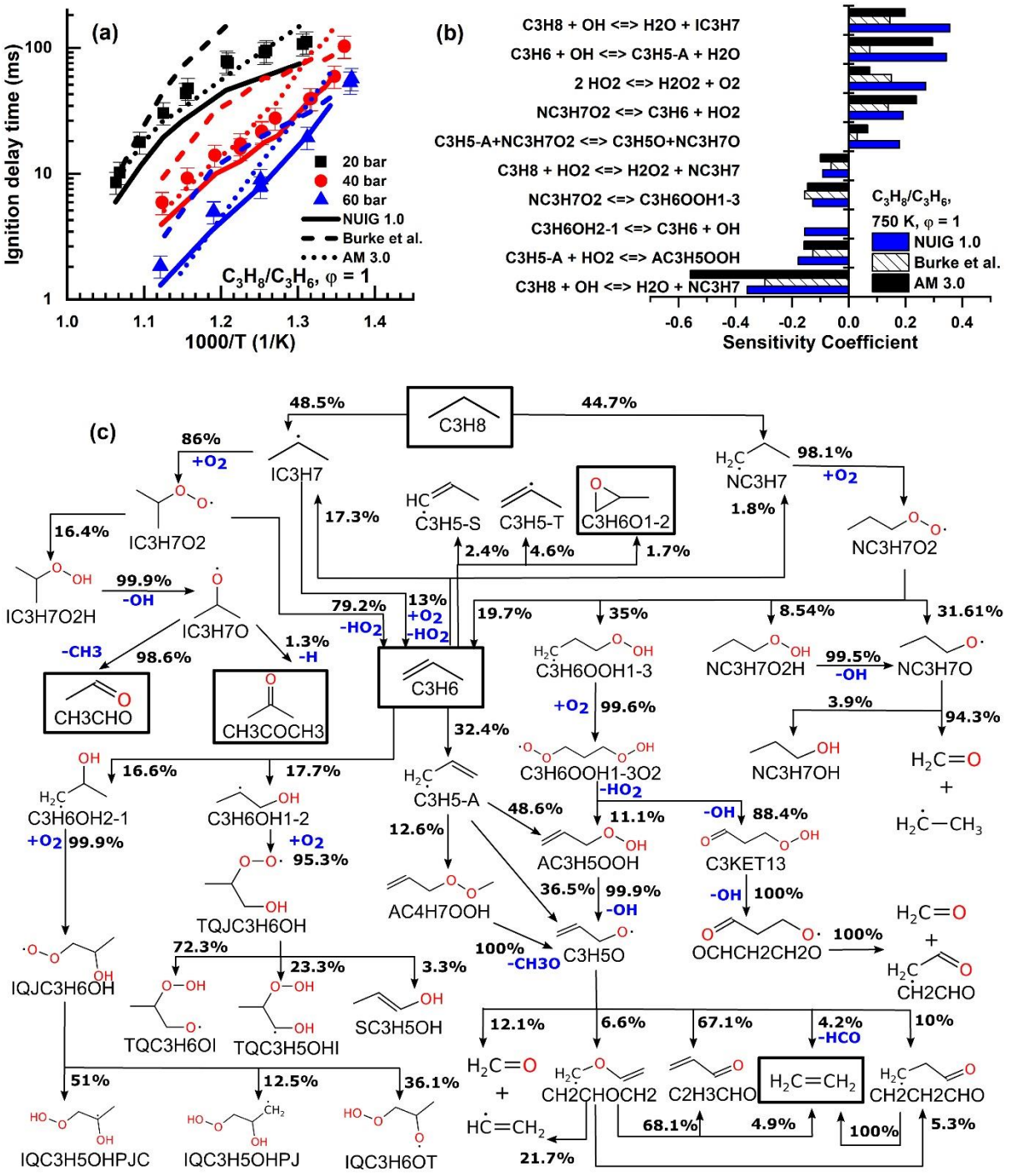


**Figure 6: (a) Performance comparison of NUIGMech1.0, the mechanism from Burke et al. [13, 14], and AramcoMech3.0 [45] with experimental IDTs at 20, 40, and 60 bar for stoichiometric conditions. (b) Sensitivity analysis on IDT using NUIGMech1.0, the mechanism from Burke et al. [13, 14], and AramcoMech3.0 for non-diluted stoichiometric propane/propene mixtures at 750 K and 40 bar. (c) Rate of production analysis using NUIGMech1.0 at 10% of the fuel (propane) consumed at conditions same as (b). The species indicated inside the rectangle are observed and quantified in the sampling experiments.**

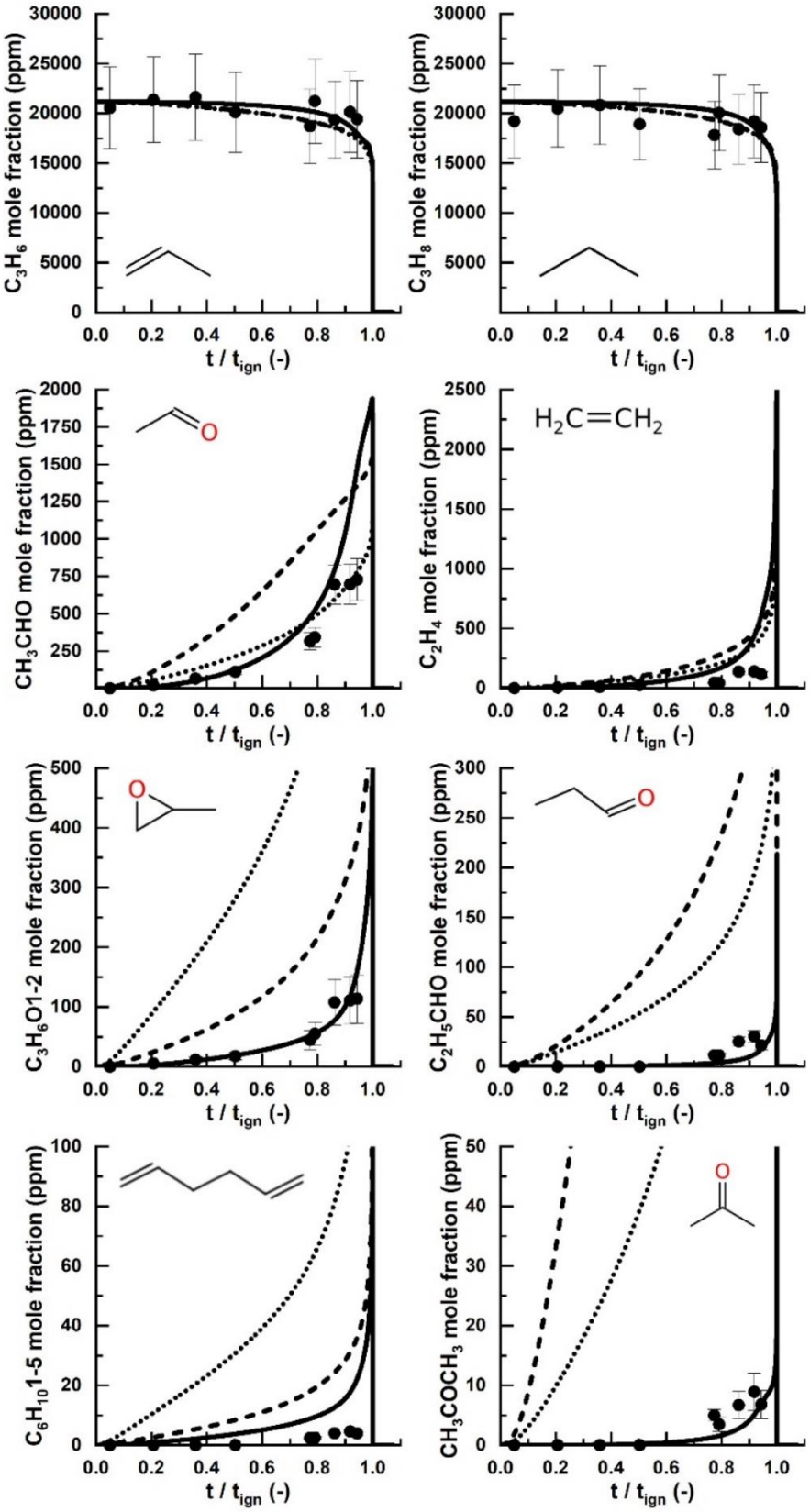


**Figure 7: Comparison of NUIGMech1.0, the mechanism from Burke et al. [13, 14], and AramcoMech3.0 [45] against the intermediate species mole fraction profiles for propane/propene oxidation at 750 K, 40 bar, and stoichiometric mixtures (Exp – symbols, Solid line – NUIGMech1.0, Dashed line – Burke et al., Dotted line – AramcoMech3.0).**

For the pressures investigated, NUIGMech1.0 can qualitatively represent the IDT measurements **(Fig 6(a)).** For the 20 bar condition, NUIGMech 1.0 over-predicts the reactivity by more than 20% in the temperature range investigated. At the 40 bar and 60 bar conditions, the performance of NUIGMech1.0 is better compared to the 20 bar predictions. The predictions differ from the experimental data by an average of 30% for the 40 and 60 bar conditions. The performance of AramcoMech3.0 [45] is qualitatively comparable to that of NUIGMech1.0 at temperatures above 820 K for the 20 and 40 bar conditions. However, at lower temperatures, the mechanism under-predicts the reactivity. In the case of Burke et al. mechanism [13, 14]**,** the reactivity is under-predicted for all of the pressures and temperatures investigated. The consumption of both propane and propene is captured well by all mechanisms (**Fig 7**). The main consumption pathway for propane is through H-atom abstraction by ȮH radicals, leading to *n*- and *iso*-propyl radicals. These pathways control reactivity in this regime, with the formation of *n*-propyl radicals promoting reactivity and *iso*-propyl radicals inhibiting reactivity and the branching ratio playing a pivotal role. The former effect is characterized by the ability of *n*-propyl radicals to undergo low-temperature chain branching pathways, whereas the latter effect is dominated by the *iso*-propyl radicals forming unsaturated species. A previous model [45] adopted the rate constant based on measurement by Droege et al. [59] over the temperature range from 298–900 K. Droege et al. [59] measured the branching ratio of *iso*-propyl and *n*-propyl in their study, and Sivaramakrishnan et al. [60] measured the total rate for $C_3H_8 + ȮH \leftrightarrow$ products. The latter study [60] applied the branching ratio obtained by Droege et al. [59] and extracted a modified Arrhenius three-parameter reaction rate constant for $C_3H_8 + ȮH$ giving *iso*-propyl + $H_2O$ and *n*-propyl + $H_2O$. Recently, Sivaramakrishnan et al. [61] used H-atom ARAS detection to quantitatively measure the concentration of H-atoms as a function of time during $C_3H_8 + ȮH$ pyrolytic experiments in an ST. The knowledge of H-atom concentrations [61] and the total rate from [60] allowed for determining the branching ratio between *iso*- or *n*- propyl formation. When comparing the two studies by Sivaramakrishnan et al. [60, 61], the recent work [61] noticed excellent agreement with their previous study [60]. **Figure 8** compares the rate constant for the $C_3H_8 + ȮH$ reaction system and the rate constant for the abstraction of the secondary C–H bond that forms $iĊ_3H_7$ radicals. The rate constant utilized in this work is the best fit for the direct measurement of $C_3H_8 + ȮH \leftrightarrow iĊ_3H_7 + H_2O$ by Sivaramakrishnan et al. [61], together with the other available experimental data. The rate utilized in NUIGMech1.0 is about 50% higher than that used in AramcoMech3.0 [45] over the high-temperature regime (1100–2000 K). The H-atom abstraction by $HȮ_2$ radicals is important at higher pressures and lower temperatures. These rate constants are adopted from the theoretical study of Aguilera-Iparraguuirre et al. [62]. However, the rate constant for the abstraction reaction forming *n*-propyl radicals has been increased by approximately 40% in the low-temperature range to agree with the measurements by Handford-Styring and Walker [63], **Fig. 9**. The study [63] measured the total rate of propane + $HȮ_2$ and utilized the bond-additivity rule to obtain the rate constant for the site specific hydrogen atom abstraction from propane.

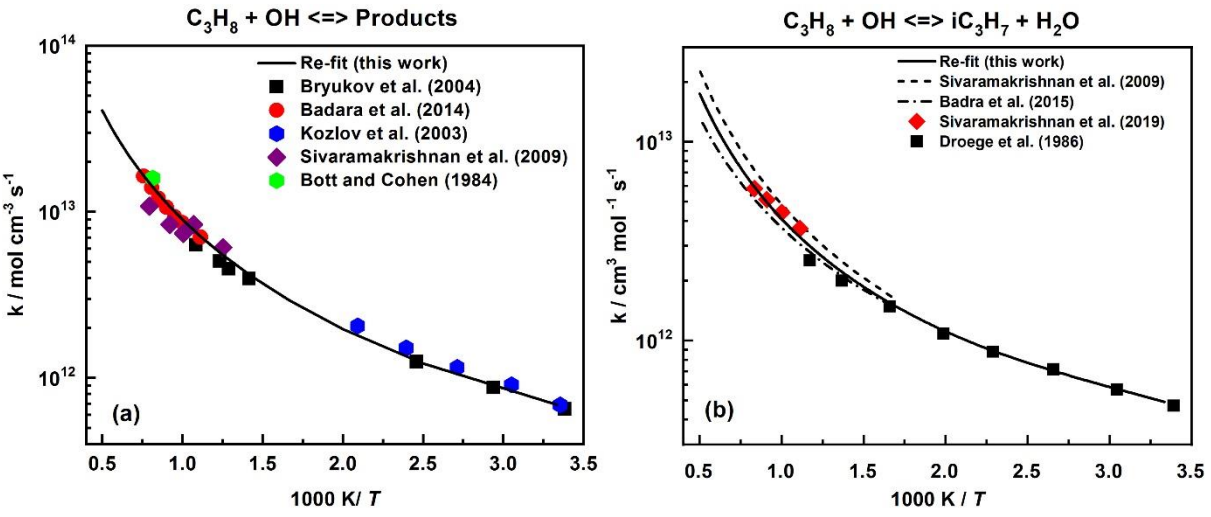

Figure 8: Plot of (a) total rate constant for $C_3H_8$ + ȮH, and (b) rate constant for the abstraction of the secondary C–H bond in $C_3H_8$ + ȮH. Comparison of current rate against the study by Bryukov et al. [64], J. Badara et al. [65], Kozlov et al. [66], Sivaramakrishnan et al. [60], [61], Bott and Cohen et al. [67] and Droege et al. [59].

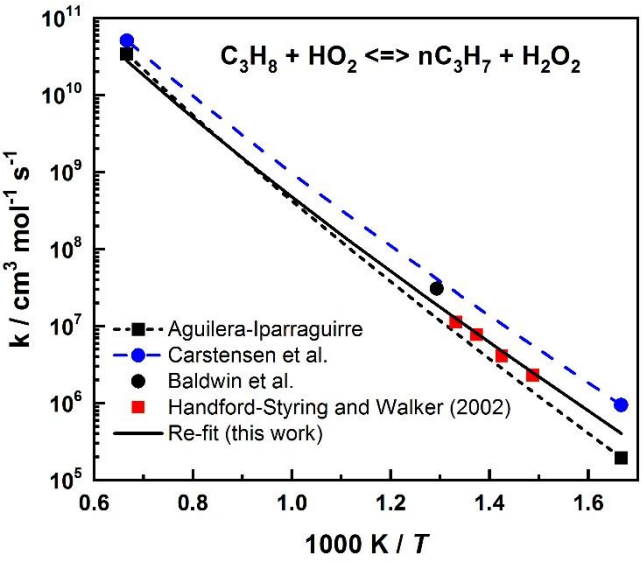


Figure 9: Rate constant comparison of $C_3H_8$+$HȮ_2$=$nC_3H_7$+$H_2O_2$ with the measured data by Handford-Styring and Walker [63], Baldwin et al. [68], along with the theoretical study of Aguilera-Iparraguirre et al. [62] and Carstensen et al. [69].

The formation of *iso*-propyl radicals and the *iso*-propyl-peroxyl radicals subsequently lead to the formation of propene. The main consumption of propene is through H-atom abstraction by ȮH radicals, leading to the formation of allyl radicals, which is also possible through H-atom abstraction from propene by hydroperoxyl, alkyl-peroxyl, and alkoxyl radicals. Other major pathways for propene consumption were discussed in Section 4.1. The consumption pathways $C_3H_6$ + ȮH ↔ $Ċ_3H_5$-a + $H_2O$, and $Ċ_3H_6$OH2-1 ↔ $C_3H_6$ + ȮH are observed to be sensitive, with the former inhibiting reactivity by consuming an ȮH radical and forming a resonantly-stabilized radical. In contrast, the latter reaction consumes an ȮH radical but undergoes subsequent chain branching pathways, thereby promoting reactivity. The formation of acetaldehyde is controlled by the Waddington pathways and also through the scission reaction of *iso*-propoxy radicals (TQ$C_3H_6$OI → $CH_2O$ + $CH_3CHO$ + ȮH, IQC3H6OT ↔ $CH_2O$ + $CH_3CHO$ + ȮH and $iC_3H_7Ȯ$ ↔ $ĊH_3$ + $CH_3CHO$). However, the ranking to their contribution is different from the pathway analysis performed for the neat propene case. The pathway leading through the *iso*-propoxy radical is more dominant in the propane/propene mixture than in the neat propene case. The reason is the abundance of the primary consumption pathway of propane.

The production of ethene is chiefly through concerted elimination reaction of ethyl-peroxyl radical. In the current mechanism, the pressure-dependent rate constant for this reaction has been updated based on the review work by Klippenstein [70] and is higher compared to the rate constant used in the previous models [13, 14, 45]. The ethyl-peroxyl radical is produced from the addition of an oxygen molecule to ethyl radical that is produced through β-scission of *n*-propoxy radicals. The other major pathways leading to the production of ethene are $Ċ_2H_5$ + $O_2$ ↔ $C_2H_4$ + $HȮ_2$, $ĊH_2CH_2CHO$ ↔ $C_2H_4$ + HĊO, and $C_3H_5Ȯ$ ↔ $C_2H_4$ + HĊO. The homolytic fission reaction class for the ketohydroperoxide has been added from the study of Goldsmith et al. [71], which is sensitive in promoting the reactivity of the fuel ($C_3$KET13 ↔ $OCHCH_2CH_2Ȯ$ + ȮH). Previously, this reaction step was lumped into one step, directly producing $ĊH_2CHO$, $CH_2O$, and ȮH radical. The branching at the second addition of molecular oxygen to hydroperoxyl-propyl radical is crucial as one pathway leads to the low-temperature chain branching ($C_3$KET13 → $OCHCH_2CH_2Ȯ$ + ȮH → $H_2CO$ + $ĊH_2CHO$), while the other pathway is mostly chain propagating, leading to the production of unsaturated compounds like acrolein and ethene ($aC_3H_5OOH$ → $C_3H_5Ȯ$ → $C_2H_3CHO$ and $C_2H_4$). In the case of propane/propene mixtures, the cross-reaction pathways play an essential role. The reaction between allyl radicals from

the propene consumption and the *n*-propyl-peroxyl radicals from the propane oxidation scheme leads to the production of *n*-propoxy and allyloxy radicals. The consumption of both radicals leads to the formation of more ethene, and therefore, contributes towards inhibiting the reactivity. Although this reaction plays a crucial role in the propane/propene case, it is not sensitive in neat propane or propene conditions. This reaction has been included in the recently developed NUIGMech1.0 and has not been investigated by quantum methods. Therefore, the rate constant has been estimated based on the work of Curran et al. [72] and optimized to fit the data for the IDT measurements. The cross-reaction influence is visible (**Fig S.3**). In the case where the cross-reaction is removed, the reactivity increases approximately by 40% at 775 K for the 40 bar condition.

The cyclic ether formation from the hydroperoxyl-propyl radical is still a substantial production route for propylene oxide. However, the governing pathway to the production of propylene oxide is through the consumption of $H\dot{O}_2$ radicals by propene to give propylene oxide and a reactive $\dot{O}H$ radical, which has been updated from work by Goldsmith et al. [71]. For this reaction, the high-pressure limit rate constant calculated by Goldsmith et al. [71] is approximately a factor of two lower than the rate constant used in the previous models [13, 14, 45]. The other pathways leading to the production of propylene oxide are through the isomerization reactions of propyl-peroxyl radicals ($nC_3H_7\dot{O}_2$ and $iC_3H_7\dot{O}_2$). The mechanism fairly represents the production of propylene oxide. The primary pathway leading to the formation of propanal is through the addition of oxygen to 1-hydroxypropen-2-yl radical ($\dot{C}_3H_6OH1\text{-}2$). The production of propanal also occurs through the reaction of *n*-propoxy radicals with molecular oxygen, where the reaction rate is adapted from the study by Zabarnick and Heicklen [55]. The production of acetone occurs mainly through the unimolecular decomposition of *iso*-propoxy radicals ($iC_3H_7\dot{O}$).

Additionally, the reactions between *iso*-propyl-peroxyl radicals ($iC_3H_7\dot{O}_2$) and smaller alkyl-peroxyl radicals ($CH_3\dot{O}_2$, $C_2H_5\dot{O}_2$) have been included in the mechanism, which contributes to the production of acetone. The predictions of both propanal and acetone species mole fractions against the experimental data show good agreement. Lastly, the 1,5-hexadiene that is majorly produced through allyl recombination is quite well captured by the mechanism in the propane/propene condition.

## 4.3 Propane

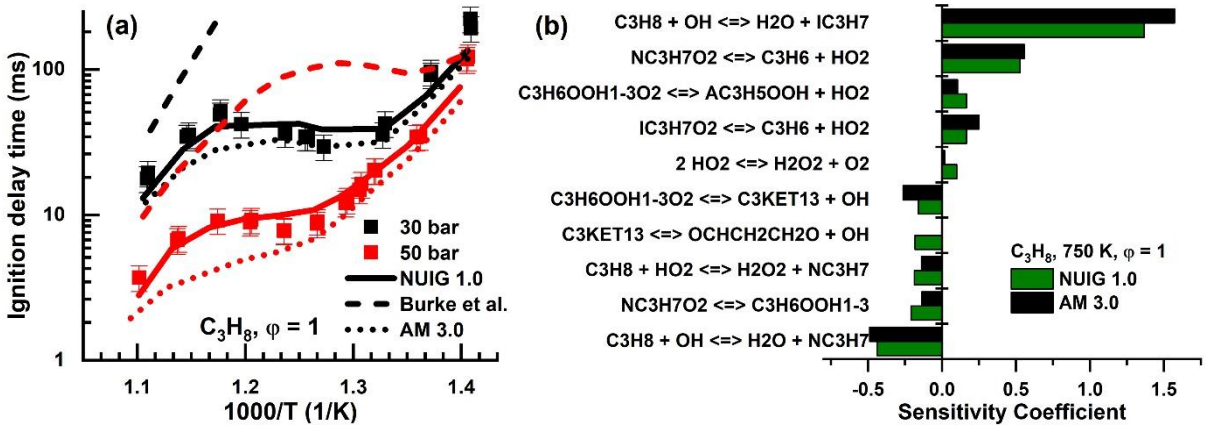


**Figure 10: (a) Performance comparison of NUIGMech1.0, Burke et al., and AramcoMech3.0 against experimental IDTs at 30 and 50 bar for stoichiometric conditions [10]. (b) Sensitivity analysis on IDT using NUIGMech1.0 and AramcoMech3.0 for non-diluted stoichiometric propane/air mixtures at 750 K, 50 bar.**

In the current study, no additional experiments on propane were performed. However, the conditions measured in the previous work on propane [10] are comparable to the conditions measured in the current study. In the work [10], ignition delay times were measured at 30 and 50 bar compressed pressure for a stoichiometric mixture. Additionally, speciation measurements were performed at 765 K and 747 K for non-diluted stoichiometric mixtures at 30 and 50 bar, respectively. The work [10] showed that AramcoMech3.0 captured the reactivity and speciation trends qualitatively better than the different mechanisms available in the literature. However, it also over predicted the

reactivity in the NTC regime for both the measured conditions. The mechanism from Burke et al. [13, 14] under predicts the reactivity of propane, and therefore, is not considered in the following discussion. Using NUIGMech1.0 leads to better predictions in the NTC regime. The improvement with the current mechanism is attributed to the combined effect of changes made in the propane sub-mechanism, as discussed in section 4.2 and the adoption of accurate values for thermo-chemistry of chemical species from ab-initio calculations computed by Goldsmith et al. [71]. **Figure 10(a)** shows the performance of NUIGMech1.0 against the experimental IDTs for propane at 30 and 50 bar. **Figure 10(b)** compares the sensitivity analysis from both of the mechanisms at 750 K for a stoichiometric mixture of propane. **Figure 11** shows a comparison of species mole fraction profiles using NUIGMech1.0 against the experimental data. As most of the detected species and their governing pathways have been discussed in Sections 4.1 and 4.2, only a brief discussion is presented here. The discussion of the updates and the kinetic analysis also establishes that the changes made to the NUIGMech1.0 have rather improved the predictions for neat propane case compared to AramcoMech3.0.

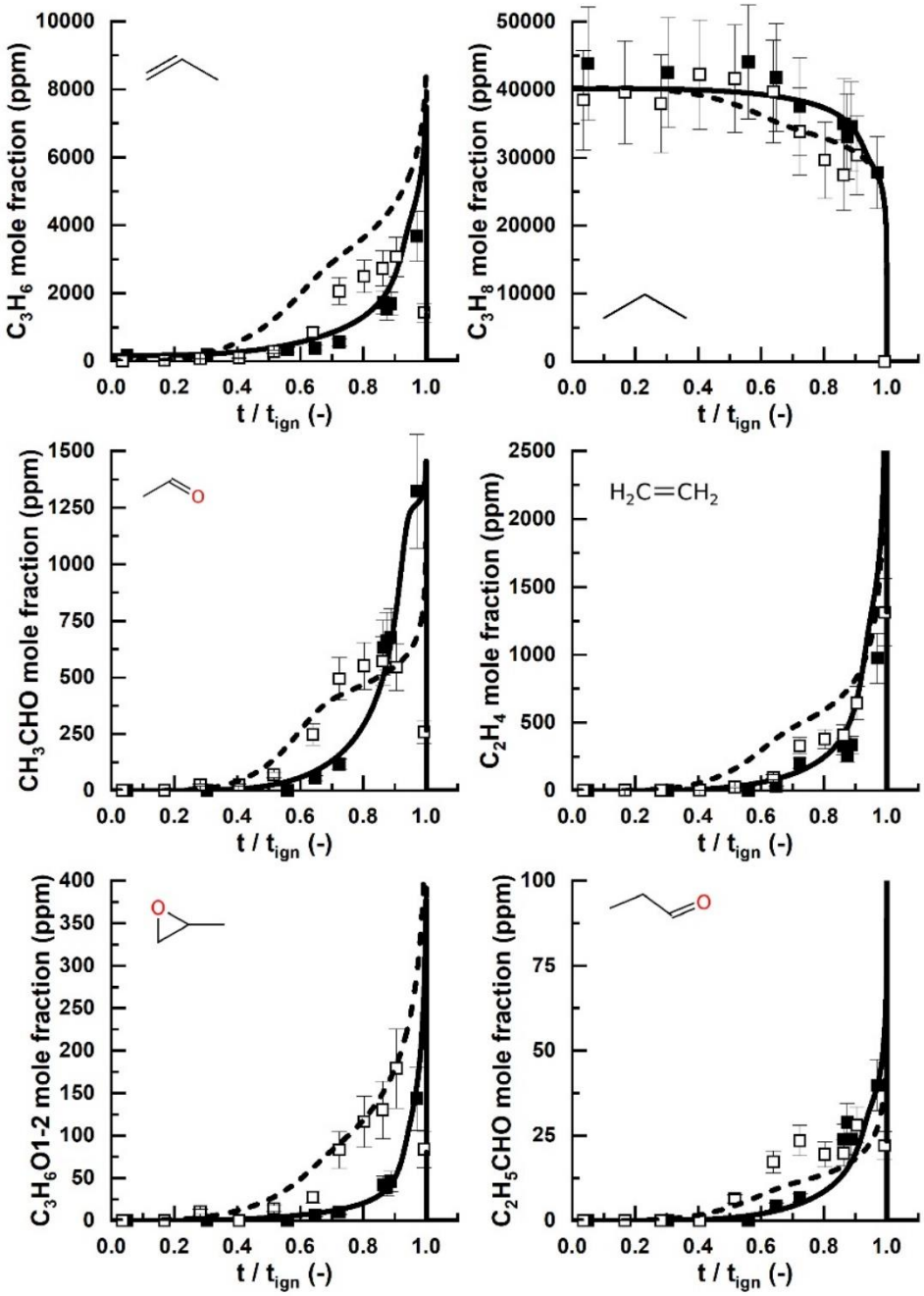


**Figure 11: Comparison of NUIGMech1.0 with the intermediate species mole fraction profiles for propane oxidation at 747 K at 50bar and 765K at 30 bar for stoichiometric mixtures (Exp. – Symbols, Filled squares – 50 bar, open squares – 30 bar; NUIGMech1.0 – Lines, solid line – 50 bar, dashed line – 30 bar).**

The consumption of propane at the investigated condition is through the H-atom abstraction by ȮH with pathway leading to *iso*-propyl radical being dominant. The optimization of the reaction rates for $C_3H_8 + ȮH \leftrightarrow nĊ_3H_7 + H_2O$ and $C_3H_8 + ȮH \leftrightarrow iĊ_3H_7 + H_2O$, as discussed in the previous section, has not influenced the consumption trend for propane. The above-discussed reactions have changed slightly from AramcoMech3.0 but have not led to any visible changes in the reactivity. The formation of propene is well predicted at 50 bar, whereas at 30 bar, the mechanism over-predicts the mole fraction profiles. The formation of propene is central, and it is mostly produced through the concerted elimination reaction of propylperoxy radicals both from the *n*- and *iso*-propyl radical pathways, with the latter pathway being dominant. Both these pathways are also sensitive in inhibiting the reactivity of the fuel. Optimizing the branching could lead to a shift in the propene predictions, but as discussed in the previous section, the branching ratio of the propyl radicals has been investigated in the

literature [59-61]. Therefore, the pressure-dependent concerted elimination reaction could be responsible for the over-estimation of the propene predictions in the 30 bar case. Similar is also the case for ethylene, which is over-predicted in the 30 bar case. Acetaldehyde is another important intermediate produced during the oxidation of propane. It is primarily formed through the β-scission of *iso*-propoxy radicals and has been updated with the reaction rate calculated by Zádor et al. [52]. Other reaction pathways leading to the formation of acetaldehyde are through the Waddington reaction pathways added to the recent NUIGMech1.0 based on the theoretical calculation by Lizardo-Huerta et al. [54]. The production pathways leading to propylene oxide and propanal have been sufficiently discussed in previous sections. The performance of the mechanism is well reflected in its predictions for both the 30 bar and 50 bar cases. A comparative illustration of the reactivity of propane, propene, and their mixtures at one common condition using constant volume simulations is provided in **SM**. The **SM** also provides a comprehensive outlook on the performance of the NUIGMech1.0 against the literature data from other reactors and experimental conditions.

The conditions investigated in the current study and from the previous study on propane allowed the validation of propane, propene, and their mixtures at comparable conditions. As the mechanism can reliably capture the reactivity at these conditions, a constant volume simulation is performed to understand the change in reactivity for the mixtures compared to the neat components. The simulation is performed at 50 bar and non-diluted stoichiometric conditions for the investigated temperature range of this study, **Fig. 12 (a)**. Propane is reactive at lower temperatures (< 800 K), followed by the mixtures and propene. However, it is observed that the ranking of the reactivity changes at temperatures above 800 K. The reactivity of the mixture is higher compared to propane and propene at higher temperatures. The nature of the NTC behavior and the reason behind the increased reactivity of the propane/propene mixtures at temperatures above 800 K is explained with sensitivity and radical pool flux analyses, **Fig. 12 (b)** and **(c).** The sensitivity analysis is performed for the three fuel mixtures at $p$ = 50 bar, $\varphi$ = 1.0, and $T$ = 900 K, while the radical pool flux analysis considers only the $\dot{O}H$ and $H\dot{O}_2$ radicals at the condition where 10% of the fuel is consumed. The radical pool flux analysis illustrates the reactions from the propane, propene, and $C_0$-$C_2$ chemistries that contribute to the production and consumption of $\dot{O}H$ and $H\dot{O}_2$ radicals.

The observed synergistic effect in reactivity for the propane/propene mixture can be explained by examining the ROP analysis of $\dot{O}H$ and $H\dot{O}_2$ in the three cases (**cf. SM**). For propane, under the conditions of interest, $H\dot{O}_2$ is formed by the direct oxidation of *iso*-propyl radical or through the concerted elimination reaction of propylperoxy radical to propene and $H\dot{O}_2$. The resulting $H\dot{O}_2$ radicals abstract hydrogen atoms from the fuel, thereby producing more $H_2O_2$, which is thermally stable at low and intermediate temperatures. At higher temperatures, $H_2O_2$ quickly decomposes to two reactive $\dot{O}H$ radicals, significantly increasing reactivity. For the neat propene system, among the reactions forming $\dot{O}H$ radicals, the fastest is the O-O bond cleavage of allylhydroperoxide, $aC_3H_5OOH$, resulting from the recombination of allyl and $H\dot{O}_2$ radicals. However, the reaction pathways forming $H\dot{O}_2$ radicals are scarce in propene, occurring via the direct oxidation of *iso*-propyl radicals, and reactions from the $C_0$-$C_2$ base chemistries. The result is a slow ignition of propene. Finally, the system of propane/propene, which shows a higher reactivity compared to neat propane and propene. As observed previously, propane has a propensity to give $H\dot{O}_2$ radicals, mainly by direct oxidation of *iso*-propyl radicals or concerted $H\dot{O}_2$ radical elimination from $iC_3H_7\dot{O}_2$. The allyl radical from propene oxidation, quickly recombines with $H\dot{O}_2$ radicals, producing $\dot{O}H$ radicals, promoting reactivity. This fast creation of $H\dot{O}_2$ radicals by propane chemistry, which rapidly converts into $\dot{O}H$ radicals governed by propene chemistry, explains the synergistic effect of propane/propene mixtures on the reactivity.

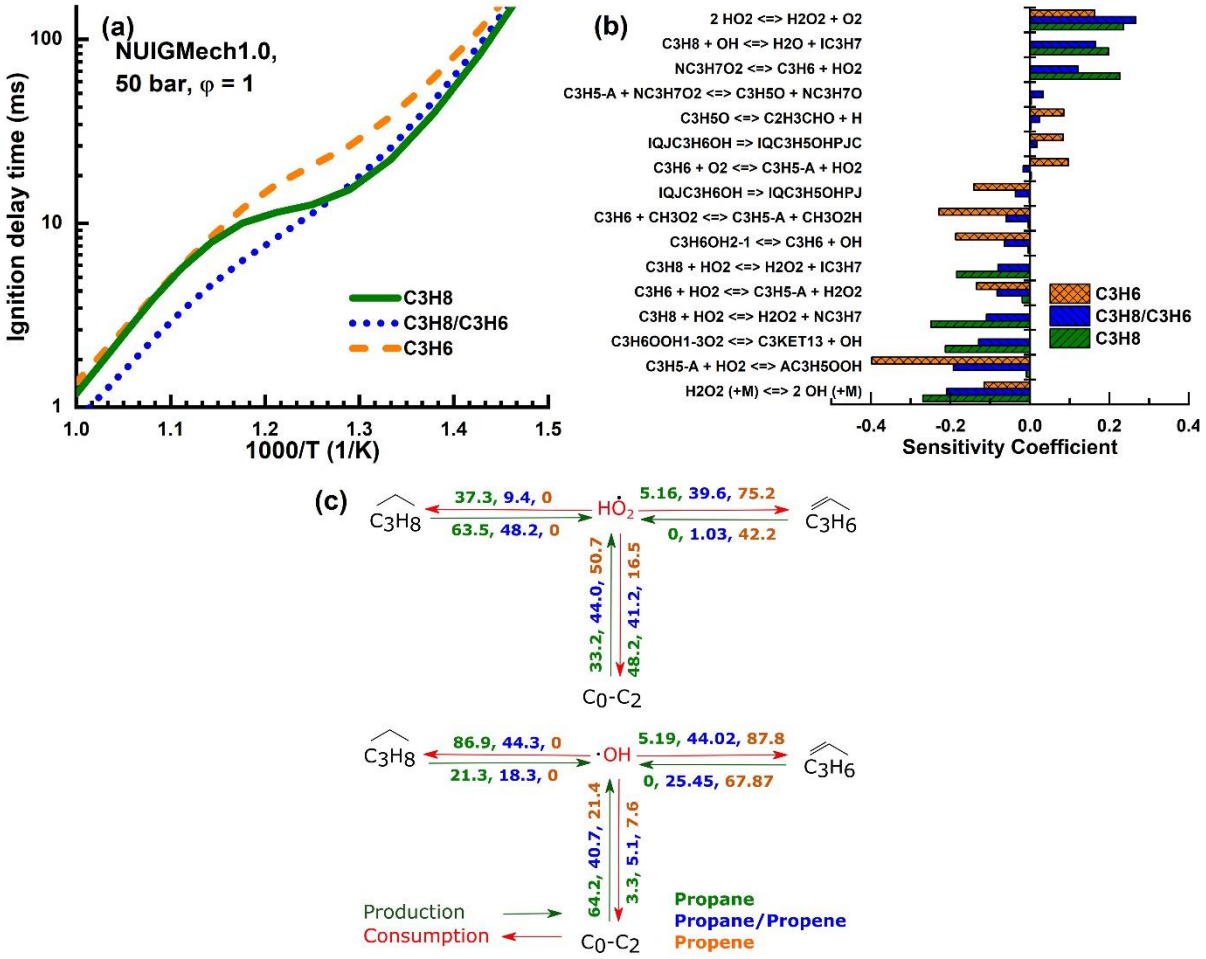


**Figure 12: (a) Constant volume simulation using NUIGMech1.0 for comparing the reactivity of propane, propene, and their mixtures at 50 bar and stoichiometric conditions. (b) Sensitivity analysis for the three fuel mixtures at 50 bar, stoichiometric condition, and 900 K. (c) Radical pool flux analysis performed at 10% of fuel consumption for the three fuel mixtures at conditions same as (b).**

To briefly summarize, NUIGMech1.0 shows an improvement in the prediction capabilities of propane, propene, and propane/propene IDTs at high pressures in the low-to-intermediate temperature regime compared to AramcoMech3.0. Concurrently, it also replicates the intermediate species mole fraction profiles in the measured conditions and also shows improvements in the data from other reactors in the literature. Overall, it can be seen that both AramcoMech3.0 [45] and Burke et al. [13, 14] mechanisms provide reasonable reactivity trends for neat components, propane, and propene, respectively. When these two mechanisms are used contrariwise, they have significant shortcomings and have to be used cautiously.

## 5. Conclusions

In the present study, IDT measurements were performed for neat components of propene and 50% propane/50% propene mixtures in an RCM at pressures ranging from 20 to 80 bar in the low-to-intermediate temperature regime. These experiments were further accompanied by novel speciation measurements for propene and propane/propene mixtures at 750 K for 40 and 50 bar conditions, respectively. The experimental work is an extension of the previous study on propane oxidation, where the speciation technique was elaborated. The combination of the two studies provides a good platform for understanding the fundamental chemical kinetic behavior of not only the neat components but also their mixtures. While the ignition delay time provides a perspective of

the reactivity of the fuel over a temperature range and pressure, the speciation measurements offer an insight into the chemistry leading to the ignition event. For the kinetic analysis of the investigated conditions, three mechanisms were considered. The different sections in the kinetic analyses reveals the strong and weak associations of the different mechanisms. The grouping of IDT and speciation measurements certainly shows that a mechanism must capture both the global and intrinsically local parameters reasonably well to have the right chemistry. This argument is evident from the kinetic analysis of both the neat components. However, to increase the confidence level on the prediction capability of the kinetic mechanism, more investigations and theoretical work is essential on aspects such as mixture variation and higher pressures. The experimental sampling technique not only proves to provide targets for mechanism development but allows investigations at high-pressure application relevant conditions. In general, NUIGMech1.0 captures the reactivity of both the neat components and the investigated mixture reasonably well. The mechanism also well predicts the recent measurements from the literature. The critical outcome of this work is the influence of cross-reactions that control the reactivity of the mixture. The reaction of allyl radicals and *n*-propyl-peroxyl radicals to form allyloxy and *n*-propoxy radicals play a crucial role in determining fuel reactivity. This reaction has not been investigated theoretically or experimentally, and the current study lays the motivation for future work targeted on binary and complex mixtures of different hydrocarbon groups.

## Acknowledgments

The authors at Physico-Chemical Fundamentals of Combustion (PCFC), RWTH Aachen University, would like to recognize the funding support from the German Research Foundation (Deutsche Forschungsgemeinschaft, DFG) through the project number – 322460823 (HE7599/2-1). The authors at Combustion chemistry center (C3), NUI Galway, would like to acknowledge the Science Foundation Ireland for funding via project numbers 15/IA/3177 and 16/SP/3829.

# Reference

[1] M. Götz, J. Lefebvre, F. Mörs, A. McDaniel Koch, F. Graf, S. Bajohr, R. Reimert, T. Kolb, Renewable Power-to-Gas: A technological and economic review, Renewable Energy 85 (2016) 1371-1390.
[2] M. Prussi, M. Padella, M. Conton, E.D. Postma, L. Lonza, Review of technologies for biomethane production and assessment of Eu transport share in 2030, Journal of Cleaner Production 222 (2019) 565-572.
[3] E. Hosseini Koupaie, S. Dahadha, A.A. Bazyar Lakeh, A. Azizi, E. Elbeshbishy, Enzymatic pretreatment of lignocellulosic biomass for enhanced biomethane production-A review, Journal of Environmental Management 233 (2019) 774-784.
[4] J. Garvey, E. Besnard, LOX-Propylene Propulsion Testing for a Nanosat Launch Vehicle, 41st AIAA/ASME/SAE/ASEE Joint Propulsion Conference & Exhibit, American Institute of Aeronautics and Astronautics2005.
[5] C. Bostwick, J. Garvey, C. Anderson, E. Besnard, Enhanced Liquid oxygen-propylene rocket engine, Vector Lauch Inc, 2018.
[6] M. Krieck, M. Günther, S. Pischinger, U. Kramer, M. Thewes, Effects of LPG Fuel Formulations on Knock and Pre-Ignition Behavior of a DI SI Engine, doi:10.4271/2015-01-1947(2015).
[7] K.J. Morganti, M.J. Brear, G. da Silva, Y. Yang, F.L. Dryer, The autoignition of Liquefied Petroleum Gas (LPG) in spark-ignition engines, Proc. Combust. Inst. 35 (2015) 2933-2940.
[8] K.J. Morganti, T.M. Foong, M.J. Brear, G. da Silva, Y. Yang, F.L. Dryer, The Research and Motor octane numbers of Liquefied Petroleum Gas (LPG), Fuel 108 (2013) 797-811.
[9] A.K. Ramalingam, M. Krieck, S. Pischinger, K.A. Heufer, Understanding the Oxidation Behavior of Automotive Liquefied Petroleum Gas Fuels: Experimental and Kinetic Analyses, Energy & Fuels, doi:10.1021/acs.energyfuels.9b03695(2020).
[10] A. Ramalingam, Y. Fenard, A. Heufer, Ignition delay time and species measurement in a rapid compression machine: A case study on high-pressure oxidation of propane, Combust. Flame 211 (2020) 392-405.
[11] S.S. Goldsborough, S. Hochgreb, G. Vanhove, M.S. Wooldridge, H.J. Curran, C.-J. Sung, Advances in rapid compression machine studies of low- and intermediate-temperature autoignition phenomena, Prog. Energy Combust. Sci. 63 (2017) 1-78.
[12] P. Sabia, M. de Joannon, G. Sorrentino, P. Giudicianni, R. Ragucci, Effects of mixture composition, dilution level and pressure on auto-ignition delay times of propane mixtures, Chem. Eng. J. 277 (2015) 324-333.
[13] S.M. Burke, U. Burke, R. Mc Donagh, O. Mathieu, I. Osorio, C. Keesee, A. Morones, E.L. Petersen, W. Wang, T.A. DeVerter, M.A. Oehlschlaeger, B. Rhodes, R.K. Hanson, D.F. Davidson, B.W. Weber, C.-J. Sung, J. Santner, Y. Ju, F.M. Haas, F.L. Dryer, E.N. Volkov, E.J.K. Nilsson, A.A. Konnov, M. Alrefae, F. Khaled, A. Farooq, P. Dirrenberger, P.-A. Glaude, F. Battin-Leclerc, H.J. Curran, An experimental and modeling study of propene oxidation. Part 2: Ignition delay time and flame speed measurements, Combust. Flame 162 (2015) 296-314.
[14] S.M. Burke, W. Metcalfe, O. Herbinet, F. Battin-Leclerc, F.M. Haas, J. Santner, F.L. Dryer, H.J. Curran, An experimental and modeling study of propene oxidation. Part 1: Speciation measurements in jet-stirred and flow reactors, Combust. Flame 161 (2014) 2765-2784.
[15] A. Burcat, K. Radhakrishnan, High temperature oxidation of propene, Combust. Flame 60 (1985) 157-169.
[16] J.-H. Choi, W.-J. Shin, W.-J. Lee, B.C. Choi, Autoignited laminar lifted flames of propene in heated coflow jets: Dependence on ignition delay time, Fuel 206 (2017) 307-317.
[17] T.L. Cong, E. Bedjanian, P. Dagaut, Oxidation of Ethylene and Propene in the Presence of CO2 and H2O: Experimental and Detailed Kinetic Modeling Study, Combust. Sci. Technol. 182 (2010) 333-349.
[18] P. Dagaut, M. Cathonnet, J.C. Boettner, Experimental study and kinetic modeling of propene oxidation in a jet stirred flow reactor, J. Phys. Chem. 92 (1988) 661-671.

[19] S.G. Davis, C.K. Law, H. Wang, Propene pyrolysis and oxidation kinetics in a flow reactor and laminar flames, Combust. Flame 119 (1999) 375-399.
[20] G. Jomaas, X.L. Zheng, D.L. Zhu, C.K. Law, Experimental determination of counterflow ignition temperatures and laminar flame speeds of C2–C3 hydrocarbons at atmospheric and elevated pressures, Proc. Combust. Inst. 30 (2005) 193-200.
[21] S. Kikui, H. Nakamura, T. Tezuka, S. Hasegawa, K. Maruta, Study on combustion and ignition characteristics of ethylene, propylene, 1-butene and 1-pentene in a micro flow reactor with a controlled temperature profile, Combust. Flame 163 (2016) 209-219.
[22] A. Movaghar, R. Lawson, F.N. Egolfopoulos, Confined spherically expanding flame method for measuring laminar flame speeds: Revisiting the assumptions and application to C1C4 hydrocarbon flames, Combust. Flame 212 (2020) 79-92.
[23] Z. Qin, H. Yang, W.C. Gardiner Jr, Measurement and modeling of shock-tube ignition delay for propene, Combust. Flame 124 (2001) 246-254.
[24] J. Shao, D.F. Davidson, R.K. Hanson, A shock tube study of ignition delay times in diluted methane, ethylene, propene and their blends at elevated pressures, Fuel 225 (2018) 370-380.
[25] M.S. Stark, D.J. Waddington, Oxidation of propene in the gas phase, Int. J. Chem. Kinet. 27 (1995) 123-151.
[26] R.D. Wilk, N.P. Cernansky, W.J. Pitz, C.K. Westbrook, Propene oxidation at low and intermediate temperatures: A detailed chemical kinetic study, Combust. Flame 77 (1989) 145-170.
[27] K. Saeed, R. Stone, Laminar burning velocities of propene–air mixtures at elevated temperatures and pressures, Journal of the Energy Institute 80 (2007) 73-82.
[28] C. Lee, S. Vranckx, K.A. Heufer, V. Khomik Sergey, Y. Uygun, H. Olivier, X. Fernandez Ravi, On the Chemical Kinetics of Ethanol Oxidation: Shock Tube, Rapid Compression Machine and Detailed Modeling Study, Z. Phys. Chem. 226 (2012) 1.
[29] A. Ramalingam, K. Zhang, A. Dhongde, L. Virnich, H. Sankhla, H. Curran, A. Heufer, An RCM experimental and modeling study on CH4 and CH4/C2H6 oxidation at pressures up to 160bar, Fuel 206 (2017) 325-333.
[30] C. Morley, Gaseq. http://www.gaseq.co.uk/.
[31] C.-J. Sung, H.J. Curran, Using rapid compression machines for chemical kinetics studies, Prog. Energy Combust. Sci. 44 (2014) 1-18.
[32] X. He, S.M. Walton, B.T. Zigler, M.S. Wooldridge, A. Atreya, Experimental investigation of the intermediates of isooctane during ignition, Int. J. Chem. Kinet. 39 (2007) 498-517.
[33] W. Ji, P. Zhang, T. He, Z. Wang, L. Tao, X. He, C.K. Law, Intermediate species measurement during iso-butanol auto-ignition, Combust. Flame 162 (2015) 3541-3553.
[34] D.M.A. Karwat, S.W. Wagnon, P.D. Teini, M.S. Wooldridge, On the Chemical Kinetics of n-Butanol: Ignition and Speciation Studies, J. Phys. Chem. A 115 (2011) 4909-4921.
[35] D.M.A. Karwat, S.W. Wagnon, M.S. Wooldridge, C.K. Westbrook, On the Combustion Chemistry of n-Heptane and n-Butanol Blends, J. Phys. Chem. A 116 (2012) 12406-12421.
[36] David G. Goodwin, Raymond L. Speth, Harry K. Moffat, B.W. Weber., Cantera: An object-oriented software toolkit for chemical kinetics, thermodynamics, and transport processes. https://www.cantera.org, 2017. Version 2.3.0., 2017.
[37] S.S. Nagaraja, J. Liang, S. Dong, S. Panigrahy, A. Sahu, G. Kukkadapu, S.W. Wagnon, W.J. Pitz, H.J. Curran, A hierarchical single-pulse shock tube pyrolysis study of C2–C6 1-alkenes, Combust. Flame 219 (2020) 456-466.
[38] M. Baigmohammadi, V. Patel, S. Martinez, S. Panigrahy, A. Ramalingam, U. Burke, K.P. Somers, K.A. Heufer, A. Pekalski, H.J. Curran, A Comprehensive Experimental and Simulation Study of Ignition Delay Time Characteristics of Single Fuel C1–C2 Hydrocarbons over a Wide Range of Temperatures, Pressures, Equivalence Ratios, and Dilutions, Energy & Fuels 34 (2020) 3755-3771.
[39] M. Baigmohammadi, V. Patel, S. Nagaraja, A. Ramalingam, S. Martinez, S. Panigrahy, A.A.E.-S. Mohamed, K.P. Somers, U. Burke, K.A. Heufer, A. Pekalski, H.J. Curran, Comprehensive Experimental and Simulation Study of the Ignition Delay Time Characteristics of Binary Blended Methane, Ethane,

and Ethylene over a Wide Range of Temperature, Pressure, Equivalence Ratio, and Dilution, Energy & Fuels, doi:10.1021/acs.energyfuels.0c00960(2020).
[40] N. Lokachari, U. Burke, A. Ramalingam, M. Turner, R. Hesse, K.P. Somers, J. Beeckmann, K.A. Heufer, E.L. Petersen, H.J. Curran, New experimental insights into acetylene oxidation through novel ignition delay times, laminar burning velocities and chemical kinetic modelling, Proc. Combust. Inst. 37 (2019) 583-591.
[41] Y. Sun, C.-W. Zhou, K.P. Somers, H.J. Curran, Ab Initio/Transition-State Theory Study of the Reactions of Ċ5H9 Species of Relevance to 1,3-Pentadiene, Part I: Potential Energy Surfaces, Thermochemistry, and High-Pressure Limiting Rate Constants, J. Phys. Chem. A 123 (2019) 9019-9052.
[42] Y. Sun, C.-W. Zhou, K.P. Somers, H.J. Curran, An ab Initio/Transition State Theory Study of the Reactions of Ċ5H9 Species of Relevance to 1,3-Pentadiene, Part II: Pressure Dependent Rate Constants and Implications for Combustion Modeling, J. Phys. Chem. A 124 (2020) 4605-4631.
[43] J. Power, K.P. Somers, C.-W. Zhou, S. Peukert, H.J. Curran, Theoretical, Experimental, and Modeling Study of the Reaction of Hydrogen Atoms with 1- and 2-Pentene, J. Phys. Chem. A 123 (2019) 8506-8526.
[44] K. Zhang, C. Banyon, U. Burke, G. Kukkadapu, S.W. Wagnon, M. Mehl, H.J. Curran, C.K. Westbrook, W.J. Pitz, An experimental and kinetic modeling study of the oxidation of hexane isomers: Developing consistent reaction rate rules for alkanes, Combust. Flame 206 (2019) 123-137.
[45] C.-W. Zhou, Y. Li, U. Burke, C. Banyon, K.P. Somers, S. Ding, S. Khan, J.W. Hargis, T. Sikes, O. Mathieu, E.L. Petersen, M. AlAbbad, A. Farooq, Y. Pan, Y. Zhang, Z. Huang, J. Lopez, Z. Loparo, S.S. Vasu, H.J. Curran, An experimental and chemical kinetic modeling study of 1,3-butadiene combustion: Ignition delay time and laminar flame speed measurements, Combust. Flame 197 (2018) 423-438.
[46] J. Badra, F. Khaled, B.R. Giri, A. Farooq, Correction: A shock tube study of the branching ratios of propene + OH reaction, PCCP 17 (2015) 24477-24477.
[47] J.F. Bott, N. Cohen, A shock tube study of the reactions of the hydroxyl radical with several combustion species, Int. J. Chem. Kinet., (1991) 1075.
[48] J. Zádor, A.W. Jasper, J.A. Miller, The reaction between propene and hydroxyl, PCCP 11 (2009) 11040-11053.
[49] C.-W. Zhou, J.M. Simmie, K.P. Somers, C.F. Goldsmith, H.J. Curran, Chemical Kinetics of Hydrogen Atom Abstraction from Allylic Sites by 3O2; Implications for Combustion Modeling and Simulation, J. Phys. Chem. A 121 (2017) 1890-1899.
[50] N.D. Stothard, R.W. Walker, Determination of the arrhenius parameters for the initiation reaction C3H6+ O2⟶ CH2CHCH2+ HO2, J. Chem. Soc., Faraday Trans. 87 (1991) 241-247.
[51] P. Barbé, F. Baronnet, R. Martin, D. Perrin, Kinetics and modeling of the thermal reaction of propene at 800 K. Part iii. Propene in the presence of small amounts of oxygen, Int. J. Chem. Kinet. 30 (1998) 503-522.
[52] J. Zádor, J.A. Miller, Unimolecular dissociation of hydroxypropyl and propoxy radicals, Proc. Combust. Inst. 34 (2013) 519-526.
[53] A. Miyoshi, Molecular size dependent falloff rate constants for the recombination reactions of alkyl radicals with O2 and implications for simplified kinetics of alkylperoxy radicals, Int. J. Chem. Kinet. 44 (2012) 59-74.
[54] J.C. Lizardo-Huerta, B. Sirjean, R. Bounaceur, R. Fournet, Intramolecular effects on the kinetics of unimolecular reactions of β-HOROO˙ and HOQ˙OOH radicals, PCCP 18 (2016) 12231-12251.
[55] S. Zabarnick, J. Heicklen, Reactions of alkoxy radicals with O2. I. C2H5O radicals, Int. J. Chem. Kinet. 17 (1985) 455-476.
[56] M.C. Flowers, Kinetics of the thermal gas-phase decomposition of 1,2-epoxypropane, J. Chem. Soc., Faraday Trans. 1 73 (1977) 1927-1935.
[57] A. Lifshitz, A. Suslensky, Shock-initiated ignition in ethylene oxide, propylene oxide, 1,2-epoxybutane, and 2,3-epoxybutane, Symp. (Int.) Combust. 25 (1994) 1571-1577.

[58] A. Lifshitz, C. Tamburu, Isomerization and decomposition of propylene oxide. Studies with a single-pulse shock tube, J. Phys. Chem. 98 (1994) 1161-1170.
[59] A.T. Droege, F.P. Tully, Hydrogen-atom abstraction from alkanes by hydroxyl. 3. Propane, J. Phys. Chem. 90 (1986) 1949-1954.
[60] R. Sivaramakrishnan, N.K. Srinivasan, M.C. Su, J.V. Michael, High temperature rate constants for OH+ alkanes, Proc. Combust. Inst. 32 (2009) 107-114.
[61] R. Sivaramakrishnan, C.F. Goldsmith, S. Peukert, J.V. Michael, Direct measurements of channel specific rate constants in OH + C3H8 illuminates prompt dissociations of propyl radicals, Proc. Combust. Inst. 37 (2019) 231-238.
[62] J. Aguilera-Iparraguirre, H.J. Curran, W. Klopper, J.M. Simmie, Accurate Benchmark Calculation of the Reaction Barrier Height for Hydrogen Abstraction by the Hydroperoxyl Radical from Methane. Implications for CnH2n+2 where n = 2 → 4, J. Phys. Chem. A 112 (2008) 7047-7054.
[63] S.M. Handford-Styring, R.W. Walker, Rate constants for the reaction of HO2 radicals with cyclopentane and propane between 673 and 783 K, PCCP 4 (2002) 620-627.
[64] M.G. Bryukov, V.D. Knyazev, S.M. Lomnicki, C.A. McFerrin, B. Dellinger, Temperature-Dependent Kinetics of the Gas-Phase Reactions of OH with Cl2, CH4, and C3H8, J. Phys. Chem. A 108 (2004) 10464-10472.
[65] J. Badra, E.F. Nasir, A. Farooq, Site-Specific Rate Constant Measurements for Primary and Secondary H- and D-Abstraction by OH Radicals: Propane and n-Butane, J. Phys. Chem. A 118 (2014) 4652-4660.
[66] S.N. Kozlov, V.L. Orkin, R.E. Huie, M.J. Kurylo, OH Reactivity and UV Spectra of Propane, n-Propyl Bromide, and Isopropyl Bromide, J. Phys. Chem. A 107 (2003) 1333-1338.
[67] J.F. Bott, N. Cohen, A shock tube study of the reaction of the hydroxyl radical with propane, Int. J. Chem. Kinet. 16 (1984) 1557-1566.
[68]

R.R. Baldwin, A.R. Fuller, D. Longthorn, R.W. Walker. In: F.J. Weinberg, editor^editors. Combustion Institute European Symposium; 1973; London: Academic Press. p. 1-70.
[69] H.-H. Carstensen, A.M. Dean, O. Deutschmann, Rate constants for the H abstraction from alkanes (R–H) by R′ O2 radicals: A systematic study on the impact of R and R′ , Proc. Combust. Inst. 31 (2007) 149-157.
[70] S.J. Klippenstein, From theoretical reaction dynamics to chemical modeling of combustion, Proc. Combust. Inst. 36 (2017) 77-111.
[71] C.F. Goldsmith, W.H. Green, S.J. Klippenstein, Role of O2 + QOOH in Low-Temperature Ignition of Propane. 1. Temperature and Pressure Dependent Rate Coefficients, J. Phys. Chem. A 116 (2012) 3325-3346.
[72] H.J. Curran, P. Gaffuri, W.J. Pitz, C.K. Westbrook, A Comprehensive Modeling Study of n-Heptane Oxidation, Combust. Flame 114 (1998) 149-177.